

Microstructural aspects of moisture adsorption of $\text{Al}_2\text{O}_3\text{-B}_4\text{C}$ compacts

K. C. RADFORD

Nuclear Materials Department, Westinghouse Research and Development Center, Pittsburgh, Pennsylvania 15235, USA

The moisture adsorption behaviour of $\text{Al}_2\text{O}_3\text{-B}_4\text{C}$ composite pellets has been studied over a wide range of fabrication variables and pellet densities. The affinity for moisture is determined primarily by the mean size of the fine pores.

1. Introduction

Composite $\text{Al}_2\text{O}_3\text{-B}_4\text{C}$ ceramic pellets are one of the prime neutron absorber materials in use for reactivity control of nuclear power reactors. Their major use is for burnable absorber applications in first cores or extended cycle reload cores, with the salient feature being that the high cross-section ^{10}B isotope in the B_4C absorbs neutrons, thus controlling the initial reactivity, and is burnt out (transmuted to the He and Li) within the first few months of operation during which time sufficient fission product inventory accumulates to naturally "poison" the fuel. Generally, the B_4C content is low, with the inert Al_2O_3 matrix being present to impart both structural support and dilution of the ^{10}B .

The importance of the moisture adsorption of the pellets is due to the fact that the absorber pellets are contained in low cross-section Zircaloy tubes to minimize the parasitic neutron absorption of the rods once the poison has fulfilled its purpose. Zircaloy has a very strong affinity for hydrogen and the potential for hydriding must be minimized to prevent failure of the rods. Unfortunately, Al_2O_3 has a strong affinity for moisture, being used extensively as a desiccant in finely powdered form, and control of moisture content is essential for satisfactory operation of the absorber rods.

To understand and control the affinity of $\text{Al}_2\text{O}_3\text{-B}_4\text{C}$ composite pellets for moisture, an investigation of the adsorption and desorption

characteristics under controlled conditions due to variations in B_4C and Al_2O_3 powder types, pellet density and microstructure was conducted. The essential features and conclusions of the investigation are reported here.

2. Experimental details

Compositions based on five B_4C and ten Al_2O_3 powders having different characteristics were made by wet mixing, drying, screening, isostatically pressing pellets and sintering under various conditions. Details of the fabrication and physical properties of the pellets are reported in another publication [1]. Pellets were also obtained from commercial suppliers*, and included one sintered composition, and three hot-pressed batches.

Moisture content was established by storing the pellets in different controlled humidity chambers for several weeks to ensure equilibration, and testing with a moisture analyser† calibrated with sodium tartrate. During testing, the pellets were held at one temperature until the counting rate decreased to background, following which the temperature was raised. The typical test temperature sequence involved 200, 300, 500 and 750°C, but other temperatures from 150 to 950°C were used to establish the kinetics of moisture evolution and the temperature necessary to completely dry the samples. High-purity argon was used as the carrier gas. Confirmatory hydrogen testing was performed by high-temperature (~1350°C) gas extraction to verify that the moisture analyser

*Boride Products, Inc., Travers City, Michigan, USA; Eagle Picher (formerly Nuclear Ceramics), Oak Ridge, Tennessee, USA.

†Dupont Instruments moisture analyser, Wilmington, Delaware, USA.

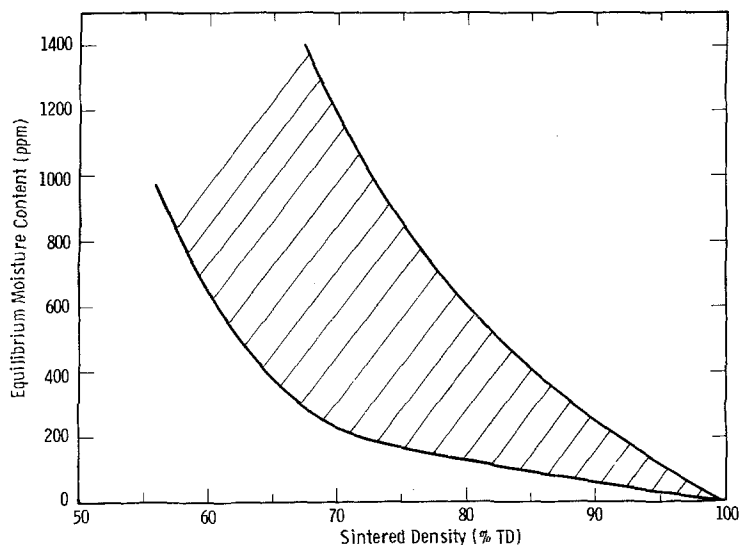


Figure 1 Moisture adsorption of $\text{Al}_2\text{O}_3\text{-B}_4\text{C}$ ceramics at 60% r.h. (75 F)*.

was operating correctly, and also to ensure that no hydrogen residue from the temporary organic binder remained after pellet sintering.

3. Results

The large number of $\text{Al}_2\text{O}_3\text{-B}_4\text{C}$ compositions ranging in density from ~60 to 93% TD (theoretical density) and containing from very fine to coarse B_4C powder in matrices prepared from moderately sinterable to highly reactive aluminas generated a considerable variation in moisture adsorbing capacity. The data could be contained within a broad band which narrowed as the density of the pellets increased, as indicated in Fig. 1. For a given density in the range 60 to 80% TD, a considerable variability in equilibrium moisture content could be obtained depending on the characteristics of the B_4C and Al_2O_3 powders involved. In general, however, most of the compositions showed similar adsorption and desorption kinetics.

All pellets rapidly adsorbed moisture from the atmosphere after sintering, and had to be dried prior to storage in the desired humidity chamber. Measurement of the equilibrium moisture content of the pellet indicated that the majority of the moisture (80 to 90%) could in all cases be removed by heating to a temperature of 300°C . The major differences occurred in moisture removal at lower temperature, with some compositions exhibiting greater moisture removal in the temperature range 150 to 200°C , whereas

others showed slightly more evolution in the range 200 to 300°C .

Moisture was retained in the pellets after drying at 300°C (i.e. 10 to 15%) which for all practical purposes could not be removed by extended drying times and required an increase in temperature, with ~5 to 15% of the total moisture being removed at 400°C and the remainder being evolved by heating to 500°C . In all cases, further heating to 600, 750 and 950°C showed practically no residual moisture after the 500°C treatment (i.e. a total further evolution < 10 ppm).

The rate of moisture evolution was extremely rapid on pellet heat up, but declined with time; this is illustrated in Fig. 2 in which 82% TD pellets were dried after exposure to both high- and low-humidity environments. Within 15 min, the moisture levels had dropped from a 150 to 250 ppm range to < 30 ppm, and further reductions proceeded at a $t^{1/2}$ rate. A flowing gas was more efficient in reducing the moisture level than a static atmosphere although the difference was slight. The kinetics of moisture removal were slightly slower after exposure to a high-humidity environment than to low-humidity.

The equilibrium moisture level increased with increasing moisture content of the environment, as shown in Fig. 3 for 82% TD pellets. Also, the attainment of equilibrium was slower at low humidities (< 2% relative) than for humidities in the 10 to 80% (relative) range in which equilibrium was achieved in times ranging from minutes

*To convert F to $^\circ\text{C}$, subtract 32 from the F value and multiply by 5/9.

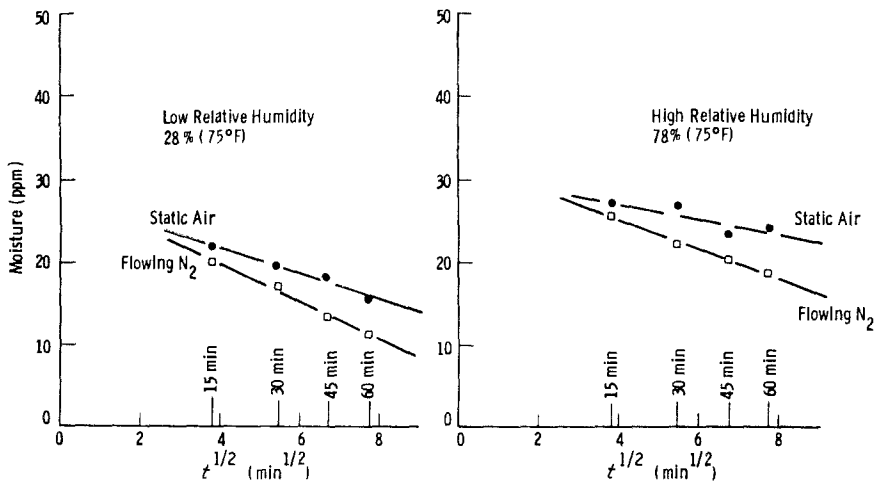


Figure 2 Reduction of moisture content of 82% TD $\text{Al}_2\text{O}_3\text{-B}_4\text{C}$ pellets with drying time at 200°C .

to a few hours, as seen in Fig. 4 for 82% TD pellets. Pellets of lower density ($\leq 75\%$ TD) adsorbed moisture more rapidly than the higher density pellets, with equilibrium being attained in a few minutes.

Pellets with densities $> 80\%$ TD showed a decrease in equilibrium moisture content with increase in density whereas the moisture capacities of lower density pellets did not follow any clear dependence on pellet density, as indicated by the increasing bandwidth in Fig. 1. These higher density pellets showed similar drying kinetics to those shown in Fig. 2, except for the highest density (93% TD) pellets which showed variable, albeit

low, moisture contents after drying for different time periods, as seen in Fig. 5, for which no consistent time-dependence could be obtained.

To understand and explain the observed moisture adsorption behaviour, and particularly the large scatter at low densities, an extensive investigation of the pellet metallography was undertaken to qualitatively evaluate the differences between samples.

Since the sintered densities of all the pellets were low, practically all the porosity was interconnected (i.e. open). Pycnometric determinations indicated that the amount of closed porosity in the samples was $\leq 1\%$ for densities as high as 81%

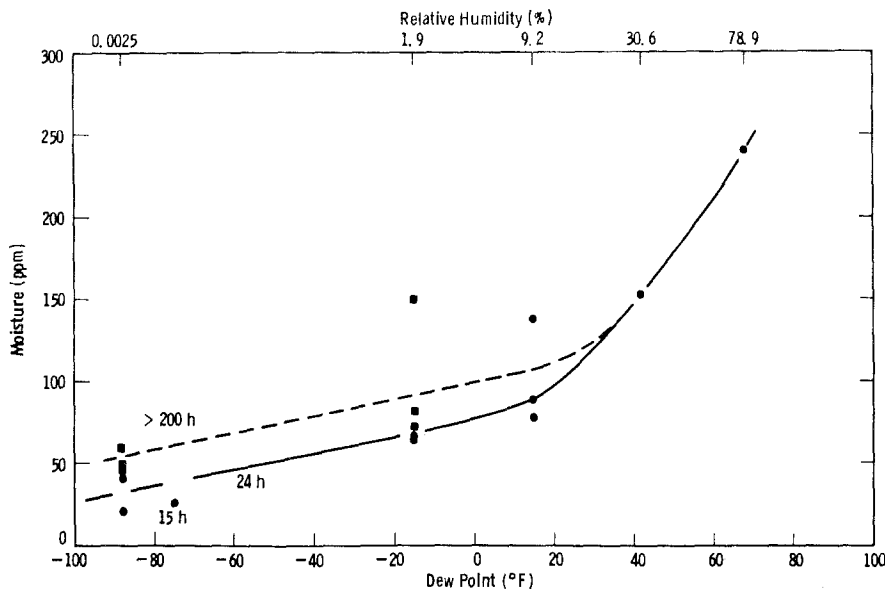


Figure 3 Equilibrium moisture content of 82% TD pellets stored at 75°F .

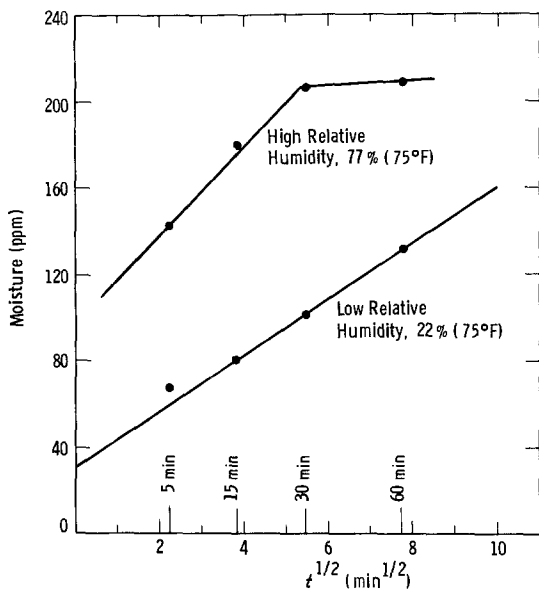


Figure 4 Moisture readorption of 82% TD sintered pellets.

TD, and increased to only ~ 5 to 7% (absolute) for pellets of 93% TD.

The open porosity varied significantly in size and distribution as shown in the selected microstructures in Fig. 6 which typify the variations seen. (The numbers correspond to the identities in Fig. 9.) It is evident that apart from the obvious differences in B_4C size and concentration among the samples, the pore morphologies are significantly different. Sample 1 shows a high-temperature sintered structure of $\sim 60\%$ TD having very open porosity channels with the matrix exhibiting a well-sintered, rounded grain structure. The size of porosity is difficult to accurately determine owing to its elongated, interconnected nature, but is estimated at between 2 and 3 μm in size. Sample 2 (66% TD) was sintered at relatively low temperature (1450°C) and the microstructure shows

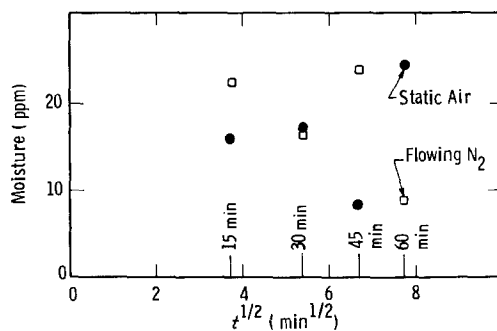


Figure 5 Drying behaviour of 93% TD $Al_2O_3-B_4C$ pellets.

a less dense matrix with the original Al_2O_3 grain structure clearly visible, and significant fine porosity evident between the grains in addition to the more obvious, coarser pores. The mean pore size is estimated to be $< 1 \mu m$. Similar evaluations of the microstructures for $\sim 70\%$ TD pellets (numbers 3 to 6) show increases in the size of the finer pores (or pore channels) with accompanying decreases in adsorptive capacity. For 80% TD pellets (numbers 7 and 8) the larger pore size of Sample 8 resulted in lower equilibrium moisture capacity, while for 93% TD material, the coarse porosity estimated at between 2 and 3 μm is consistent with the measured moisture properties.

To quantify these observed differences in microstructure, selected samples were evaluated by mercury porosimetry to establish the differences in pore sizes. The samples studied showed substantial differences between them as illustrated by the two porosimeter traces shown in Fig. 7 for samples of approximately the same density. (The samples are identified in Fig. 9 by letters.) In all cases the pore volume was predominantly monosized, with the mean size varying as shown in Table I. In addition to the intrusion porosimetry

TABLE I Comparison between mercury porosimetry and calculated pore sizes

Composition identity	Immersion density ($g\ cm^{-3}$)	Measured moisture (ppm)	Mercury porosimetry av. pore size (μm)			Calculated pore size (μm)
			Intrusion	Hysteresis	Average	
A	68.0	1420	0.2	0.7	0.5	0.38
B	69.5	880	0.4	0.8	0.6	0.58
C	78.3	508	0.45	1.15	0.8	0.71
D	77.1	205	1.1	3.5	2.3	1.86
E	67.4	240	1.7	2.0	1.85	2.26
F	70.9	200	1.5	2.3	1.9	2.43
G	70.4	125	1.8	5.5	3.65	3.47
H	63.1	159	2.0	4.5	3.25	3.87

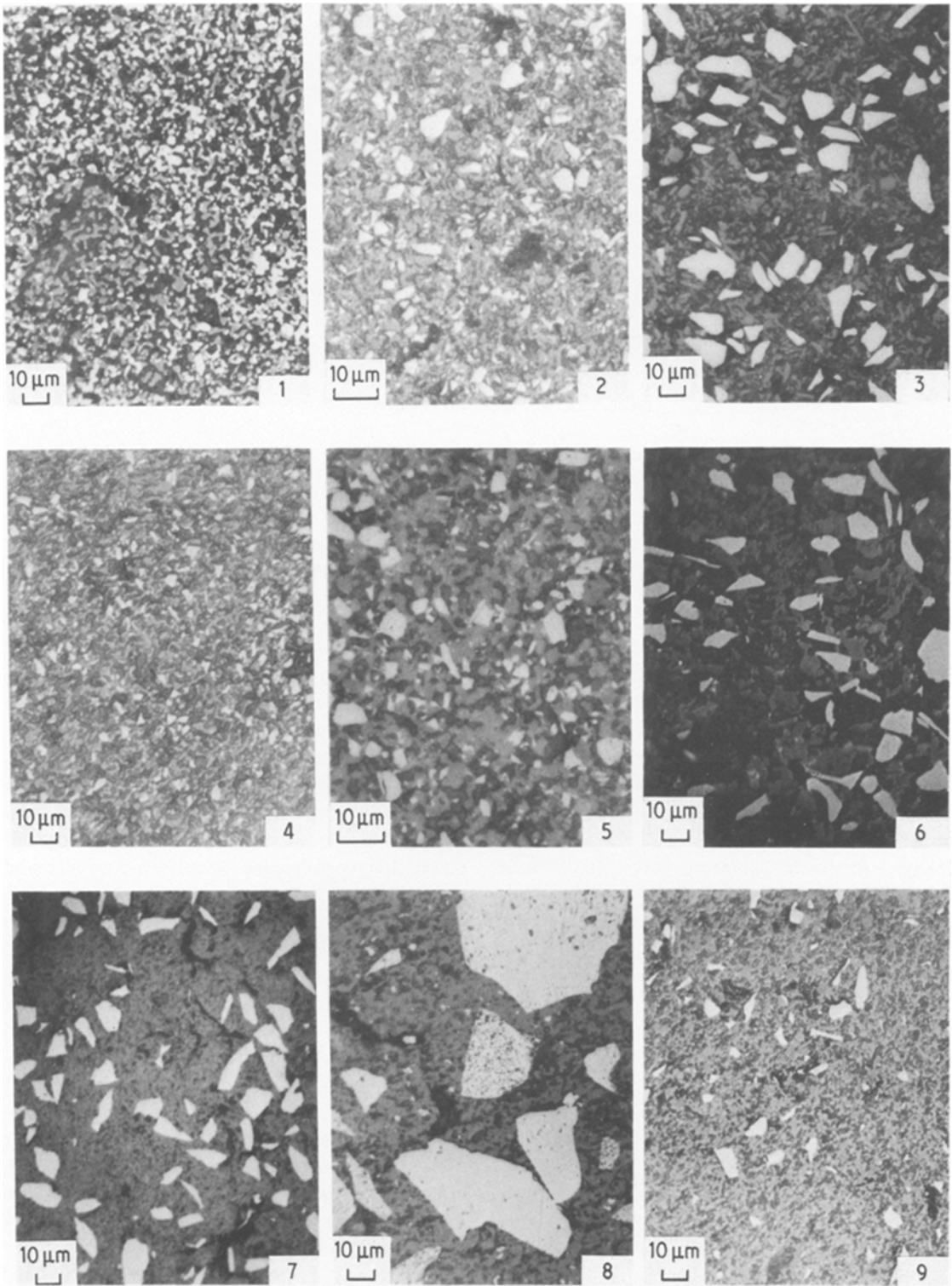


Figure 6 Photomicrographs of representative $\text{Al}_2\text{O}_3\text{-B}_4\text{C}$ structures identified in Fig. 9. See text for sample details.

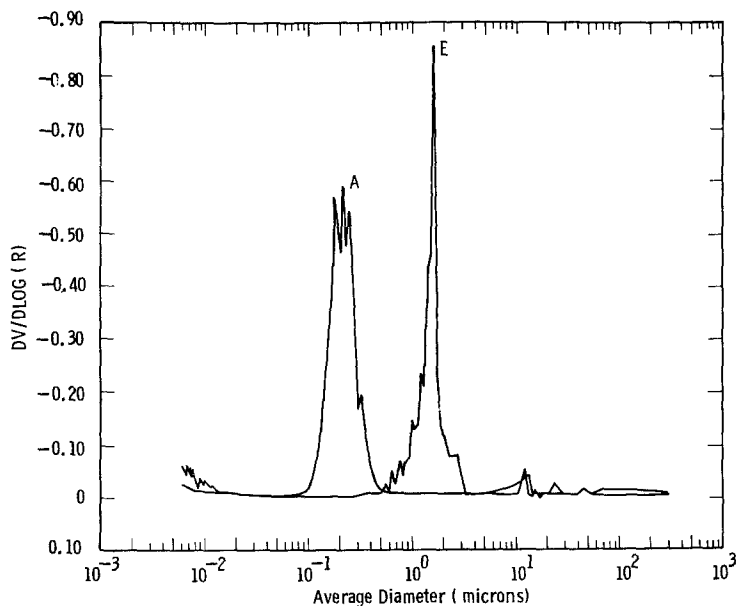


Figure 7 Comparison of mercury intrusion porosimetry results for $\text{Al}_2\text{O}_3\text{-B}_4\text{C}$ samples A and E.

data, hysteresis information was obtained which again indicated a monosized pore distribution, but displaced in size as shown in Table I. This hysteresis behaviour is frequently observed and has been ascribed to an "ink bottle" type of pore structure [2, 3] which requires forcing the mercury through a narrow neck into the body of the pore which is assumed spherical.

It is possible to rationalize the observed moisture behaviour, at least qualitatively, in terms of the size of the porosity which is a measure of the available surface for adsorption, and the sample density. Assuming spherical pores, it is easily shown that the available surface area is inversely proportional to the diameter (d) of the pore for a given void volume (V) by the amount $6V/d$. A good correlation was observed for a 70% TD pellet between the measured 1000 ppm moisture content and the amount predicted by assuming a monomolecular film, an area for the water molecule of 10.51 \AA^2 (0.1051 nm^2) derived using the equation [3]

$$A = 1.091 \left(\frac{M}{\rho N} \right)^{2/3} \times 10^{16}$$

where M is the molecular weight, N Avogadro's number, and ρ the density, and monosized pores $0.5 \mu\text{m}$ in size as determined by mercury porosimetry. The agreement, within a factor of 2, is excellent considering that in reality a distribution of pore sizes exists, and that the finer pores have a much stronger influence on the surface available

for adsorption, and implies that the moisture adsorption in this pellet is indeed a monomolecular layer.

Using this approach, the moisture adsorption can be predicted for any density and pore size giving results as shown in Fig. 8 which indicates the strong dependence of moisture capacity on porosity for small pore sizes. Superimposing the pore-size dependence of moisture adsorption on the data, it is possible to explain the wide scatter in the results by categorizing the data into mean pore size classes, as shown in Fig. 9. A very good correlation between the calculated pore size and the average of the mercury porosimetry intrusion and hysteresis pore sizes (Table I) can also be seen in Fig. 9, lending credence to the theory that moisture adsorption in these ceramics is due to a monolayer and is controlled predominantly by the average pore size of the material which dictates the surface area available for adsorption.

Confirmation of the pore-size dependence of moisture adsorption was obtained from surface-area measurements. Samples of $\sim 77\%$ TD pellets which had been resintered indicated little change in sintered density, but exhibited a large decrease in surface area from 1.15 to $0.82 \text{ m}^2 \text{ g}^{-1}$ and a corresponding decrease in moisture adsorption from 756 to 222 ppm. Mean pore-size calculations (based on spherical pores) provided values of 0.40 and $1.37 \mu\text{m}$, respectively (identified in Fig. 9 by +), which are in good agreement with the predicted values described by the lines for the different pore sizes.

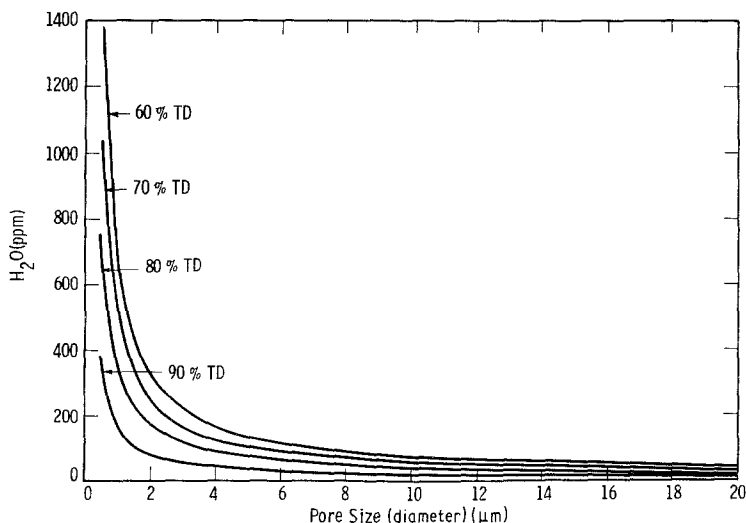


Figure 8 Calculated moisture adsorption in $\text{Al}_2\text{O}_3\text{-B}_4\text{C}$ pellets as a function of mean pore size.

4. Discussion

Moisture adsorption in $\text{Al}_2\text{O}_3\text{-B}_4\text{C}$ pellets is determined mainly by the surface properties of the Al_2O_3 matrix. Experiments with well-sintered, low-density B_4C pellets have shown substantially less adsorptive capacity, and the kinetics are much slower than for the composite material. This behaviour is not surprising, since the strong desiccating action of alumina is well known [4]. Adsorption is a property possessed by all solids to some degree and arises from unbalanced surface forces or valences of the surface molecules [4]. Highly polar molecules, such as water, are strongly attracted, and the amount of adsorption is expected to depend strongly on the available surface.

Studied by Ervin and Osborn [5] showed that low surface area, $\alpha\text{-Al}_2\text{O}_3$ did not show any

rehydration, although other studies on $\alpha\text{-Al}_2\text{O}_3$ [6] having high surface area (40 to $70\text{ m}^2\text{ g}^{-1}$) indicated hydration to boehmite and diaspore. Since the surface areas of the current samples were all moderately low, it is considered that the possibility of hydrate formation is minimal. However, it has been found [7] that oxycarbide formation, which is a possible reaction product of B_4C containing excess carbon and Al_2O_3 , is very sensitive to moisture, and adsorbs significant quantities. It is also possible for the B_4C particles to react with water [8] forming H_3BO_3 , although the kinetics for this reaction at room temperature are considered to be very slow. Since the electron microprobe did not detect evidence of reaction of Al_2O_3 and B_4C , it is considered that the oxycarbide contribution is negligibly small, and that

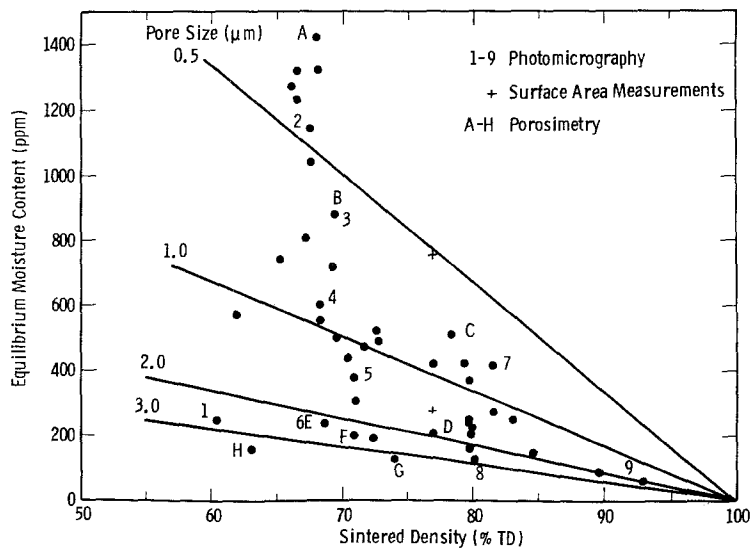


Figure 9 Classification of $\text{Al}_2\text{O}_3\text{-B}_4\text{C}$ moisture adsorption with mean pore size and pellet density.

the predominant mode of water retention in these pellets is by adsorption on Al_2O_3 surfaces.

The kinetics of adsorption and desorption appear to be diffusion controlled, evidence for which is given by the $t^{1/2}$ relationships observed. This type of behaviour is expected based on the microstructures in which the water molecules have to diffuse down the open pore channels into the body of the pellets. The rapid desorption behaviour is indicative of predominantly physically adsorbed moisture, but the lack of total desorption at temperatures $< 200^\circ\text{C}$, and the observation that some compositions exhibited greater desorption than others at temperatures $> 200^\circ\text{C}$ implies the possibility of chemisorption of the water molecule. De Boer *et al.* [9] reported that chemisorbed moisture is proportional to the specific surface area, amounting to 248 ppm m^{-2} which implies the binding of one water molecule to two oxygen atoms in the surface. Based on this criterion, it is considered that chemisorption is not of prime importance in these $\text{Al}_2\text{O}_3\text{-B}_4\text{C}$ pellets, since it would account for approximately 90% of the observed moisture adsorption. Also, the low temperatures needed for removal of the majority of the moisture are not consistent with chemisorption although it probably constitutes a certain percentage, particularly in those samples having low densities and high moisture levels.

Since temperatures of the order of 500°C are required to remove trace moisture, it is also possible that some hydrate formation may occur, although it is more probable that this reflects the increased energy necessary to remove the moisture from the fine capillaries in the body of the pellet. The variable desorption behaviour of the 93% TD pellets is believed to be due to the tortuous paths of the interconnected fine capillaries which made more difficult the equilibration of the vapour pressure within the pores and the external surface.

From the variety of B_4C and Al_2O_3 powders studied, it is concluded that the moisture capacities of the pellets are not so much dependent on the size of the B_4C particles or the sintering activities of the Al_2O_3 powders *per se*, but reflect the final microstructure, and particularly the fine pore content in the structure. The decrease in equi-

librium moisture content with increase in density reflects not only the fact that the total pore content decreases, but also that the higher density structures contain larger, more rounded pores having less surface than structures sintered at lower temperatures, which is consistent with the sintering of all ceramic bodies. The data indicates that the attainment of an $\text{Al}_2\text{O}_3\text{-B}_4\text{C}$ pellet having low density and low moisture adsorption capacity is achievable, and requires that the structure contain fine pores having rounded, well-sintered topography of low surface area. The average pore size required is dictated by the moisture adsorption-pore size relationship as shown in Fig. 9.

5. Conclusions

Moisture adsorption and desorption in $\text{Al}_2\text{O}_3\text{-B}_4\text{C}$ pellets is diffusion-controlled, and adsorption capacity is inversely related to density. There does not appear to be a correlation between capacity and either size, shape or volume fraction of the B_4C , or to the properties of the Al_2O_3 powder *per se*. The moisture adsorption behaviour is consistent with a monolayer coverage of the available (open) surface, which can be related primarily to the size of the fine pores.

References

1. K. C. RADFORD, *J. Mater. Sci.* **18** (1983) 669.
2. C. ORR, *Powder Technol.* **3** (1969-70) 117.
3. S. J. GREGG and K. S. W. SING, "Adsorption, Surface Area and Porosity" (Academic Press, London, 1967).
4. W. H. GITZEN (ed), "Alumina as a Ceramic Material" (American Ceramic Society, 1970).
5. G. ERVIN and E. F. OSBORN, *J. Geol.* **59** (1951) 381.
6. H. KRISHNER and K. TORKAR, *Sci. Ceram.* **1** (1962) 63.
7. L. M. FOSTER, G. LONG and M. S. HUNTER, *J. Amer. Ceram. Soc.* **39** (1) (1956) 1.
8. E. S. BYRON, J. F. THOMPSON and S. W. POREMBKA, "Solubility of Enriched Boron and Boron Compounds", WAPD-BT-6 (1958) pp. 23-26.
9. J. H. DE BOER, J. M. H. FORTUIN, B. C. LIPPENS and W. H. MEIJS, *Koninkl. Ned. Akad. Wetenschap. Proc.* **57B** (1954) 434.

Received 21 June
and accepted 12 July 1982